Miner Petrol (2009) 96:81–98
DOI 10.1007/s00710-008-0040-3

ORIGINAL PAPER

Xenoliths of dunites, wehrlites and clinopyroxenites in the basanites from Batoke volcanic cone (Mount Cameroon, Central Africa): petrogenetic implications

P. Wandji · J. P. F. Tsafack · J. M. Bardintzeff ·
D. G. Nkouathio · A. Kagou Dongmo · H. Bellon ·
H. Guillou

Received: 26 May 2008 / Accepted: 17 December 2008 / Published online: 13 January 2009

Abstract The lavas of the Mount Cameroon, a Plio-Quaternary stratovolcano and the most important volcano along the Cameroon Volcanic Line (CVL), constitute a weakly differentiated alkaline series: mainly comprising basanites as well as alkaline basalts, hawaiites and mugearites. Ultramafic xenoliths (1–5 × 0.5–4 cm) of dunites, wehrlites and clinopyroxenites have been discovered in the basanites of a strombolian cone, located near Batoke on the South flank of the massif at an elevation of 500 m. K-Ar whole rock dating of the basanitic host rock has yielded an age of 0.73 ± 0.08 Ma. This result falls within the range of the seven new K-Ar age determinations of mafic lavas, between 2.83 Ma and the Present. These are the first K-Ar data on this massif. The $^{87}Sr/^{86}Sr$ ratios of basic lavas are low (0.703198–0.703344), and $^{143}Nd/^{144}Nd$ ratios are intermediate (0.512851–0.512773). These ratios are typical of a mantle origin. The main characteristics of the xenoliths are: (a) total FeO contents are 15.1 to 19.1 wt.% in olivines (chrysolite, Mg# ranging from 79 to 84) of xenoliths, and 4.7 to 6.9 wt.% in diopsides of xenoliths, (b) diopsides of the clinopyroxenites have up to 7.2 wt.% Al_2O_3 and 2.3 wt.% TiO_2, (c) spinels occur as interstitial grains between chrysolite and diopside grains, i.e. Cr_2O_3-rich magnetites (19 to 21 wt.% Cr_2O_3) in the dunites as well as (22 to 25 wt.% Cr_2O_3) in the wehrlites and titanomagnetites (14 to 15 wt.% TiO_2) in the clinopyroxenites. Mineralogical analyses show an important re-equilibration between the chrysolite xenocrysts and the

Editorial handling: A. Möller

P. Wandji
Laboratoire de Géologie,
École Normale Supérieure,
Université de Yaoundé I,
BP 47 Yaoundé, Cameroun
e-mail: pierrewandji@yahoo.fr

J. P. F. Tsafack
Département des Sciences de la Terre,
Faculté des Sciences, Université de Yaoundé I,
BP 812 Yaoundé, Cameroun
e-mail: ftsafack2000@yahoo.fr

J. M. Bardintzeff (✉)
Laboratoire de Pétrographie-Volcanologie, bât. 504,
Université Paris-Sud,
91405 Orsay Cédex, France
e-mail: jacques-marie.bardintzeff@u-psud.fr

J. M. Bardintzeff
IUFM, Université de Cergy-Pontoise,
95000 Cergy-Pontoise, France

D. G. Nkouathio · A. Kagou Dongmo
Département des Sciences de la Terre, Faculté des Sciences,
Université de Dschang BP 67,
Dschang, Cameroun

D. G. Nkouathio
e-mail: nkouathio@yahoo.fr

A. Kagou Dongmo
e-mail: kagoudongmo@yahoo.fr

H. Bellon
UMR CNRS 6538, IUEM, Laboratoire de Géochronologie,
Université de Bretagne Occidentale,
6 av. Le Gorgeu,
CS 93637, 29238 Brest Cédex 3, France
e-mail: herve.bellon@univ-brest.fr

H. Guillou
CNRS, LSCE,
Av de la Terrasse,
91198 Gif sur Yvette, France
e-mail: herve.guillou@lsce.ipsl.fr

host basanitic magma. We observed a decrease in Mg and Ni towards the rim, and an enrichment in all others cations like Fe, Mn, Ca, Si. The changes of Fe^{2+} / Mg^{2+} are the most important. The xenoliths are interpreted as cumulates: clinopyroxenite xenoliths have probably crystallized and fractionated at an early stage from the mafic (host basanitic) magma, while dunite and wehrlite xenoliths seem to have crystallized from a previous more primitive batch of magma. These alkaline liquids could have been derived from partial melting of a garnet- rich lherzolite in the upper mantle beneath the Cameroon Volcanic Line. The Al^{IV}/Al^{VI} ratios remain high (1.2 to 4.9) in the clinopyroxenes of the xenoliths. This suggests crystallization under a lower pressure than that of equilibration of the clinopyroxenes (ratios 0.6 to 0.8) found in typical mantle xenoliths from the CVL.

Introduction

Mount Cameroon is the highest volcanic massif within the continental segment of the Cameroon Volcanic Line (CVL) (Fig. 1). This huge stratovolcano culminates at 4,095 m. The CVL is made up of 12 main volcanic centres with ages ranging from 51.8 Ma to the Present (Fitton and Dunlop 1985; Ménard et al. 2002; Fosso et al. 2005; Déruelle et al. 2007; Moundi et al. 2007). The most recent eruptions were those of 1999 and 2000 on Mount Cameroon (Déruelle et al. 2000; Wandji et al. 2001; Suh et al. 2003), and the emanation of lethal gas from Lake Monoun in 1984 and Lake Nyos in 1986 (Kusakabe et al. 1989; Wandji et al. 1994). Among the ca. 140 strombolian cones that are scattered over the Mount Cameroon area, a hundred are located on the southern, south-eastern and south-western

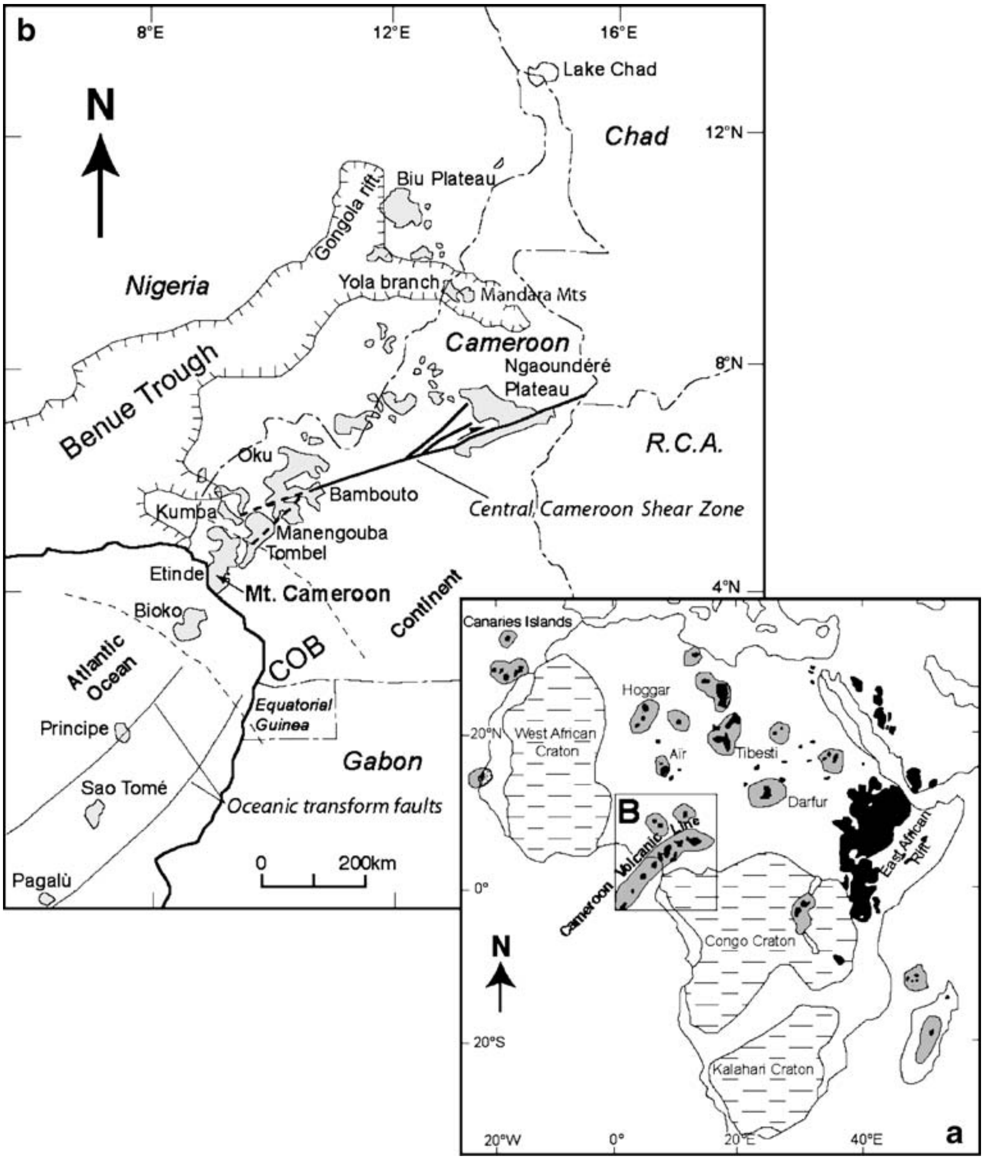

Fig. 1 **a** Location map of the Cameroon Volcanic Line (CVL). The main geologic features of Africa are indicated. **b** Location of Mount Cameroon and other main volcanic centres along the Cameroon Volcanic Line (modified according to Nkouathio et al. 2008). COB Continental Ocean Boundary. Dashed lines are limits between the CVL segments: ocean, COB and continent

plunging towards the Atlantic Ocean flanks of the volcano.

Ultramafic xenoliths (dunites, wehrlites, and clinopyroxenites) were collected on one of the southern strombolian cones, at an elevation of 500 m near Batoke (Fig. 2). Similar xenoliths (wehrlite and clinopyroxenite, 15 cm in diameter) have already been discovered in pyroclastic deposits (alkaline basalt) of another strombolian cone at 3,000 m elevation on the northwest flank of Mount Cameroon (Déruelle et al. 2001; Ngounouno et al. 2001).

Other outcrops with xenoliths have already been identified in Cameroon. Dautria and Girod (1986) described lherzolite xenoliths from a Quaternary volcano at Dibi, Northern Adamawa, near the rift of Ngaoundere, containing 63–81 vol.% olivine, 12–18 vol.% orthopyroxene, 6–16 vol.% clinopyroxene, and moreover spinel and plagioclase. Nana (2001) and Temdjim et al. (2004) studied peridotite xenoliths in recent alkali basalts at Lake Nyos: these are mostly lherzolites and harzburgites with scarce olivine-websterites. Teitchou et al. (2007) observed typical lherzolites in the Kumba Plain near Mount Cameroon, with 58–69 vol.% olivine, 14–26 vol.% orthopyroxene, 11–17 vol.% clinopyroxene, and 1–5 vol.% spinel. Lee et al. (1996) studied xenoliths (harzburgites and lherzolites) from several places in Cameroon. Princivalle et al. (2000) studied the clinopyroxenes of lherzolites from Lake Nji. Caldeira and Munha (2002) discussed the petrology of ultramafic nodules from Sao Tomé Island: these included harzburgites and lherzolites, dunites, orthopyroxenites as well as clinopyroxenites and olivine clinopyroxenites (see below).

The aim of this study is to describe the petrographical, mineralogical and geochemical character of the xenoliths and their relations to their host lavas, in order to determine their origin. The interpretation of the associated magmatic process will allow us to propose a model for the petrogenetic evolution of the basanites and then their relations with xenoliths.

Geological framework

Mount Cameroon is a part of the CVL tectonic structure which is the consequence of a series of parallel faults oriented N30 (Burke and Whiteman 1973). From the distribution of the cones scattered on the massif, three major tectonic axes that control the volcanic activity could be identified: the Batoke axis (030° to 040°), the Debundscha axis (060° to 070°) and the Limbe axis (140° to 150°).

Mount Cameroon is a large stratovolcano intercalated between the Tombel graben to the north and the Douala basin to the south. Its elliptical base measures 50 km in length by 35 km in width. Morphologically, it looks like a horst with prominent boundary faults that can be traced along breaks of slopes (Déruelle 1982). Its basement (Pan-African granites and gneisses) is covered by Cretaceous to Quaternary sediments (Dumort 1968; Tsafack et al. 2007).

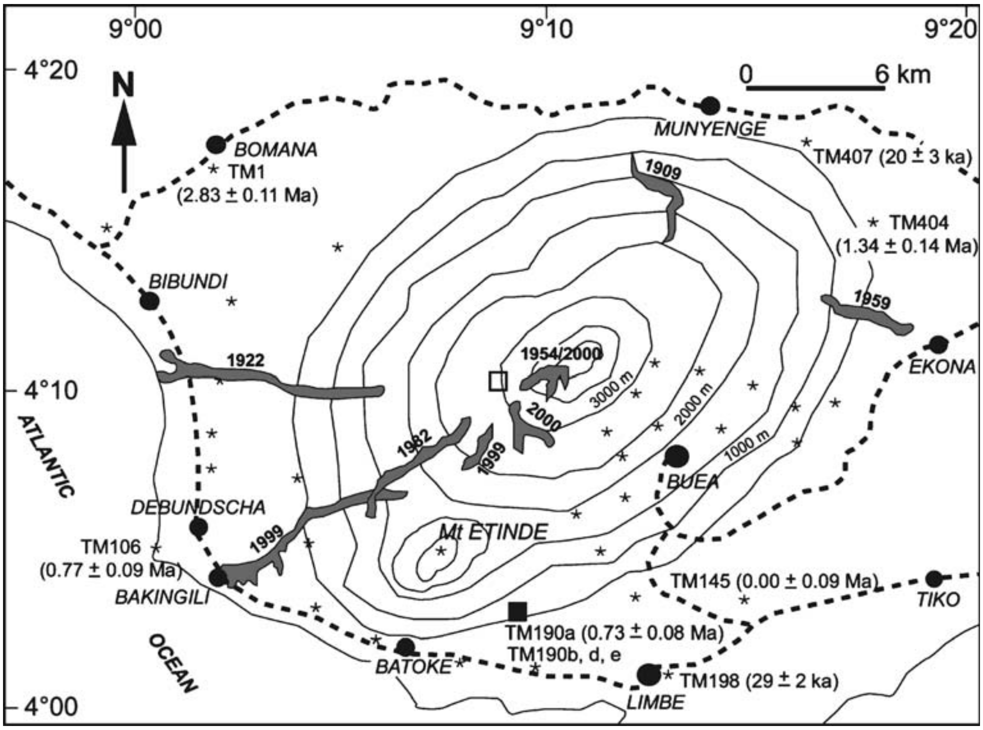

Fig. 2 Sampling map. Recent lava flows are represented in black and the years of eruption are indicated, including the most recent of 1999 and 2000. Stars indicate lava samples and ages are indicated in brackets. Filled square indicates xenoliths and the host basanite (this study) located 500 m above the sea level. Empty square indicates xenoliths collected at 3,000 m above sea level (Déruelle et al. 2001). Elevations are indicated. Roads are represented by thick, discontinuous lines

Different types of volcanic activity have been identified:

- Important effusive eruptions produced lava flows that tend to be thick, chaotic. Many are bounded by levees, that are natural banks of chilled material channelling the lava into a self-made channel (Francis 1993);
- Important explosive eruptions alternated with effusive eruptions. Pyroclastic deposits are several meters thick, sometimes more. As a result, intercalated massive lava flows and thick tephra layers have progressively built the stratovolcano. Statistically, pyroclastic deposits have built more than the half of the volcanic massif;
- Moderate explosive activity has built numerous strombolian cones; today, about 140 cones are scattered on the whole massif;
- Exceptional hydromagmatic activity is responsible for two maars: one is located at Debundscha and the other is the maar of Mount Bomana in the sedimentary basement at the North West flank of the volcano (Fig. 2).

Mount Cameroon lavas are mainly basanites (60%), alkali basalts (20%), hawaiites (12%) and less common mugearites (8%). Moreover, camptonites, which are a type of lamprophyre, composed mainly of plagioclase and brown hornblende, have been described by Ngounouno et al. (2006).

The xenoliths described in this paper were collected from a small strombolian cone at an elevation of 500 m, between 4°02′ and 4°04′ North and between 9°08′ and 9° 10′ East on the Limbe axis. This cone has a height of about 70 m and a diameter of 600 m. Blocks of xenolith-rich basanites are abundant within 300 m of the base.

Analytical methods

Lavas and xenoliths have been analysed at the Centre de Recherches Pétrographiques et Géochimiques (CRPG) at Nancy, France. Major element analyses have been made by ICP-OES (Inductively Coupled Plasma - Optical Emission Spectrometry) and trace element analyses by ICP-MS (Mass Spectrometry). During preparation of the samples, about 300 mg of powder have been treated with $LiBO_2$ and dissolved in HNO_3. Five international geostandards have been used (basalt BR, diorite DRN, serpentinite UBN, anorthosite ANG and granite GH, Carignan et al. 2001).

Minerals have been analysed with CAMECA SX 50 or SX 100 (15 kV, 10 nA) electron microprobes at Université Pierre et Marie Curie, Paris VI, France. Kα lines were used. Standards are diopside for Si, Ca and Mg, Fe_2O_3 for Fe, $MnTiO_3$ for Ti and Mn, Cr_2O_3 for Cr, albite for Na, orthoclase for K and Al, counting times are 10 s for Pk (peaks) and 10 s for Bg (background), with a 5 µm defocused beam.

Isotopic analyses were made by D. Demaiffe at the Laboratoire de Géochimie Isotopique, Université Libre de Bruxelles, Belgium, with a Micromass VG 54 multi-collector thermal-ionisation mass spectrometer. Sr isotopic ratios are corrected for mass fractionation with normalization to $^{86}Sr/^{88}Sr=0.1194$. Replicate analyses of the NBS 987 standard yielded an average $^{87}Sr/^{86}Sr$ value of 0.710255± 10. Nd isotopic data are corrected for mass fractionation by normalization to ratio $^{146}Nd/^{144}Nd=0.7219$. Replicate analyses of the La Jolla Nd standard gave an average $^{143}Nd/^{144}Nd$ value of 0.511854±8.

Whole rock K-Ar ages were determined at the Laboratoire de Géochronologie, Université de Bretagne Occidentale, Brest, France, following the analytical procedure detailed in Bellon and Rangin (1991). The samples were crushed and sieved to 0.30–0.15 mm grain size. Alteration products were eliminated by sifting, washing in distilled water and passing through the ultra-sound cleaner at the Université Paris-Sud Orsay. The grained fraction was used for argon extraction by high frequency heating under high vacuum. Isotopic composition of argon and concentration of radiogenic argon ($^{40}Ar^*$) were measured with mass spectrometry. Part of the granular fraction was crushed to a powder in an agate mill. K contents of whole rock were measured by atomic absorption spectrometry on acid solutions realized after a chemical attack of the powders in sealed polycarbonate bottles with hydrofluoric acid (HF) at 70°C during 12 h. Constant values of Steiger and Jäger (1977) have been used for age calculations. Uncertainties have been calculated using equations of Mahood and Drake (1982) and are given at 1 σ.

Two samples, TM198 and TM407 were K-Ar dated, using an unspiked technique described by Charbit et al. (1998). This technique differs from the conventional isotope dilution method in that argon extracted from the sample is measured in sequence with purified aliquots of atmospheric argon at the same working gas pressure in the mass-spectrometer. This allows percentages of radiogenic argon ($^{40}Ar^*/^{40}Ar_T$) as small as 0.14% to be measured (Scaillet and Guillou 2004). Combined with a high within-run signal stability (maximum ratio drift around 1‰), this permits individual samples of 40–50 ka basalt containing 2 wt.% K_2O to be dated with an analytical precision of ±2 ka on a single-run basis (2σ). Groundmass was separated from fresh samples following the methods of Guillou et al. (1998). Phenocrysts and xenocrysts which are potential carriers of extraneous ^{40}Ar were eliminated using magnetic, gravimetric, and visual hand picking. Replicate unspiked K-Ar age determinations were done on the microcrystalline groundmass of the two samples. The determination of K was carried out by atomic absorption with a relative precision of 1%. Argon was extracted by radio frequency heating of 1.0–2.5 g of sample, then transferred to an ultrahigh-vacuum glass line and purified with titanium sponge and Zr-Ar getters. Isotopic analysis were performed using a 180°, 6 cm radius mass spectrometer with an accelerating potential of 620 V. The atmospheric correction is monitored via two separate measurements of atmospheric argon for each sample. A first atmospheric argon aliquot is measured at the same gas pressure as the sample, and serves as an isotopic reference for the determination of its radiogenic content under identical mass-discrimination conditions. The second aliquot measured is a calibrated volume of atmospheric Ar, used to convert beam intensities to atomic abundances. As both reference aliquots (isotopic and manometric) are atmospheric in composition, they provide a cross check on the radiogenic composition of the sample. Periodic cross-calibration of zero-age standards precisely constrains the mass-discrimination to within ±0.5‰ on the ^{40}Ar/^{36}Ar ratios. The manometric calibration is based on periodic, replicate determinations of international dating standards of known K-Ar age using the same procedure for the unknowns as described in Charbit et al. (1998). This allows the total ^{40}Ar content of the sample to be determined with a precision of about ±0.2% (2 σ). Uncertainties for the K and Ar data are 1 σ analytical only, and consist of propagated and quadratically averaged experimental uncertainties arising from the K, ^{40}Ar (total), and ^{40}Ar* determinations. Uncertainties on the ages are given at 2 σ.

Petrography and mineralogy of xenoliths

(1) Host lava

The host lava outcrops as discontinue blocks of porphyritic vesicular basanites. The basanites are rich in euhedral phenocrysts and angular xenocrysts of olivine (chrysolite) and diopside and contain xenoliths. Resorption of some chrysolite xenocrysts has reduced them to skeletal shape.

The matrix contains fine microcrysts of chrysolite, clinopyroxene, Fe-Ti oxides and plagioclase. Glass is rare. Reaction rims between the host basanitic liquid and the xenocrysts resulting from re-equilibration are not observable under the microscope, but are revealed by electron microprobe analyses.

Olivine phenocrysts of the host lava have chemical compositions of chrysolite, decreasing from Fo$_{81}$ in the cores to Fo$_{75–80}$ at their rims. The microcrysts have compositions of Fo$_{75}$ which are similar to those at the rim of phenocrysts. Hyalosiderite is found in other mafic lavas of the Mount Cameroon. The clinopyroxenes of the host basanite are diopsides rich in TiO$_2$ (2 to 4 wt.%) and CaO (22 wt.%) but differ from fassaites described by Wandji et al. (2000) in the Noun Plain. They have compositions of Wo$_{49–46}$En$_{36–42}$Fs$_{10–15}$ and their Mg# = Mg/(Mg+Fe) vary from 71 to 80. Their Cr$_2$O$_3$ contents are about 0.06 wt.% for the phenocrysts and 0.12 wt.% for the xenocrysts. The oxides are titanomagnetites with TiO$_2$ contents varying from 19 to 23 wt.% and contain a high percentage of ulvöspinel component (52 to 62 wt.%). FeO$_t$ contents range from 61.8 to 65.6 wt.%.

(2) Chrysolite xenocrysts

Chrysolite xenocrysts in the host basanite have compositions ranging from Fo$_{81–84}$ in their cores to Fo$_{75–83}$ at their rims. Electron microprobe analyses show significant re-equilibration between the chrysolite xenocrysts and the host basanitic liquid (Table 1). It is marked by decreasing Mg^{2+} and Ni^{+} and by an increase of all the others cations such as Fe^{2+}, Mn^{2+}, Ca^{2+}, Si^{4+} in the xenolith rim. The exchanges of Fe^{2+}/Mg^{2+} between chrysolite xenocrysts and the liquid are the most important. Rims of xenocrysts are richer in Fe^{2+} than the cores (increase of 2.06%) as well as Si, Mn (increase of 66.7%), and Ca and poorer in Mg, Ni (Table 1).

(3) Xenoliths

Three types of xenoliths are found in the basanite: dunites, wehrlites and clinopyroxenites. They are 0.5 to 4 cm wide and 1 to 5 cm in length. They contain three mineral phases: olivine (chrysolite), clinopyroxene (diopside) and spinel (Tables 2, 3 and 4).

Table 1 Evidence for re-equilibration of chrysolite xenocryst with host basanite from element zoning profiles

cations	165 core	166 rim	tendency	cationic variation	cationic variation (in %)	variation vs core content (in %)
Si	0.983	0.986	increasing	+0.003	10	+0.30
Fe $^{2+}$	0.340	0.347	increasing	+0.007	23.33	+2.06
Mn	0.006	0.010	increasing	+0.004	13.33	+66.66
Mg	1.657	1.644	decreasing	−0.013	43.33	−0.78
Ni	0.005	0.003	decreasing	−0.002	6.67	−40
Ca	0.008	0.009	increasing	+0.001	3.33	+12.5
Total	2.999	2.999		0.03	99.99	

3. a. Dunites

More or less rounded dunite xenoliths measure 3 to 5 cm in diameter. They are composed (visually) of 91% chrysolite, 7% diopside and 2% spinel (Fig. 3). Dunites have a porphyroclastic texture (sample TM190b, Fig. 4a) with typical kink-bands in chrysolites, that suggest that some degree of deformation has affected these rocks. The size of their grains ranges from 0.8 to 1.6 mm for the chrysolites and from 2 to 4 mm for the diopsides. Under the microscope, the contact between the xenolith and host basanite has a rusty colour attributable of alteration.

Chrysolites ($Fo_{83–84}$) have the same composition as the cores of the xenocrysts. Diopsides have compositions of $Wo_{47–46}En_{43–44}Fs_{9–10}$ (Fig. 5). Spinels are mostly interstitial between grains of chrysolite, and some are as inclusion in chrysolites. Cr_2O_3 contents are about 20 wt.%, for Al_2O_3 contents of 10 wt.%, and MgO contents of 7 wt.%; Cr# (= Cr / Cr + Al) and Mg# are respectively 57 to 58 and 31 to 32. FeO_t contents vary between 52 and 54 wt.% (Fig. 6, Table 4).

3. b. Wehrlites

Wehrlites are composed of a granular assemblage (0.4–2 mm) of crystals of chrysolite (78%), diopside (21%) and spinel (1%). They show granular and porphyroclastic textures (sample TM190e, Fig. 4b). The olivines are cracked. The clinopyroxenes occupy spaces between chrysolite minerals. Spinels are found mostly as inclusions in chrysolite and rarely occupy the interstices between the grains.

Chrysolites are Fo_{81}. CaO contents of the chrysolites of wehrlites (0.2–0.3 wt.%) are nearly the same as those of the dunites (0.1–0.4 wt.%) and are higher (Table 2) than those from the mantle (0.05–0.1 wt.%) (Lee et al. 1996). This probably reflects an equilibrium environment under a lower pressure (Caldeira and Munha 2002). Clinopyroxenes ($Wo_{47–45}En_{43–46}Fs_{8–9}$) of the wehrlites are almost identical to those analyzed in dunites (Fig. 5). They are diopsides with Mg# values similar to those of chrysolites (81–84), except in the case of some diopsides that have relatively high Mg# values of 85 to 86. They are Cr-rich, with a Cr_2O_3 contents reaching 1.2 wt.%. Spinels have relatively constant compositions in terms of FeO_t (41.9 to 43.3 wt.%), Cr_2O_3 (22.7 to 25.3 wt.%), MgO (6.2 to 9.7 wt.%) and Al_2O_3 (16 to 19 wt.%). Cr# and Mg# values are 45 to 50 and 40 to 43 respectively (Fig. 6, Table 4).

3. c. Clinopyroxenites

Clinopyroxenite xenoliths have sizes ranging from 0.5 to 1 cm. They are composed of 95% diopside, 4% chrysolite and 1% titanomagnetite and have a mosaic equigranular texture according to Mercier and Nicolas (1975) (sample TM190d, Fig. 4c). The mineral sizes are 0.4 to 0.7×0.3 to

Table 2 Representative microprobe analyses of chrysolites from the host basanite and xenoliths

Rock	host basanite							dunite					wehrlite			clinopyroxenite	
Sample	TM190a							TM190b					TM190e			TM190d	
Analysis	165x.c	166x.b	168ph.c	177ph.b	170m	188ph.b	189ph.c	1	4	8	9	296	97	102	106	318	327
SiO2	38.64	38.71	40.29	39.75	39.40	38.95	40.59	40.37	39.66	39.94	40.10	40.53	40.15	39.89	39.90	39.07	38.76
TiO2	0.04	0.05	0.06	0.12	0.05	0.04	0.09	0.00	0.02	0.13	0.13	0.02	0.05	0.04	0.06	0.00	0.00
FeO	16.00	16.28	17.82	19.90	22.42	22.41	16.53	15.25	16.31	16.07	15.08	16.26	17.29	17.98	17.96	17.33	20.73
MnO	0.26	0.47	0.27	0.35	0.32	0.35	0.14	0.50	0.35	0.23	0.09	0.32	0.34	0.22	0.11	0.39	0.25
MgO	43.71	43.28	41.81	40.17	38.27	38.42	43.53	43.60	44.13	43.97	44.26	43.47	41.84	42.21	42.01	42.29	40.15
NiO	0.24	0.13	0.18	0.25	0.33	0.01	0.25	0.27	0.27	0.22	0.23	0.19	0.26	0.08	0.29	0.28	0.13
CaO	0.29	0.33	0.09	0.19	0.39	0.35	0.20	0.16	0.12	0.13	0.09	0.18	0.20	0.30	0.21	0.27	0.10
Total	99.18	99.25	100.52	100.73	101.18	100.53	101.33	100.15	100.86	100.69	99.98	100.97	100.13	100.72	100.54	99.63	100.12
Si	0.98	0.99	1.02	1.01	1.02	1.01	1.02	1.02	0.99	1.00	1.01	1.01	1.02	1.01	1.01	1.00	1.00
Ti	0.00	0.00	0.00	0.00	0.00	0.00	0.00	0.00	0.00	0.00	0.00	0.00	0.00	0.00	0.00	0.00	0.00
Fe2+	0.34	0.35	0.38	0.42	0.48	0.49	0.35	0.32	0.34	0.34	0.32	0.34	0.37	0.38	0.38	0.37	0.45
Mn	0.01	0.01	0.01	0.01	0.01	0.01	0.00	0.01	0.01	0.00	0.00	0.01	0.01	0.00	0.00	0.01	0.01
Mg	1.66	1.64	1.58	1.53	1.47	1.49	1.62	1.64	1.65	1.64	1.66	1.62	1.59	1.60	1.58	1.61	1.54
Ni	0.00	0.00	0.00	0.01	0.01	0.00	0.01	0.01	0.01	0.00	0.00	0.00	0.01	0.00	0.01	0.01	0.00
Ca	0.01	0.01	0.00	0.01	0.01	0.01	0.01	0.00	0.00	0.00	0.00	0.01	0.01	0.01	0.01	0.01	0.00
Total	3.00	3.00	3.00	2.99	3.00	3.00	3.00	3.00	3.00	3.00	3.00	2.99	3.00	3.00	2.99	3.01	3.00
Fo	82.6	82.0	80.2	78.1	75.0	74.9	82.2	83.2	82.5	83.0	83.8	82.2	80.7	80.8	80.6	80.9	77.0

Number of cations calculated on the basis of 3. x: xenocryst, ph: phenocryst, c: core, b: rim, m: microcryst (analyses at Université Paris VI for Tables 2, 3, 4)

Table 3 Representative microprobe analyses of diopsides from the host basanite and xenoliths

Rock	Host basanite				dunite		wehrlite					Clinopyroxenite		
Sample	TM190a				TM190b		TM190e					TM190d		
Analysis	163ph.c	164ph.b	171x.c	172x.b	43	44	99	100	101	111	146	76	77	78
SiO2	47.23	45.45	49.63	48.53	50.62	51.39	51.39	52.28	51.66	52.39	51.06	48.91	49.54	48.39
TiO2	2.90	3.99	2.00	2.53	1.43	1.23	0.99	0.73	0.91	0.78	1.42	1.96	1.73	1.93
Al2O3	5.76	8.12	5.83	5.14	4.37	3.91	4.19	3.27	3.69	3.22	4.52	5.57	5.69	6.33
Cr2O3	0.06	0.06	0.14	0.10	0.37	0.44	0.89	1.21	0.96	1.02	0.98	0.33	0.29	0.34
FeOt	7.96	8.20	6.20	8.05	5.95	5.62	5.61	4.78	4.72	4.74	5.62	6.06	6.52	6.86
MnO	0.00	0.12	0.06	0.16	0.17	0.30	0.00	0.18	0.02	0.00	0.09	0.00	0.00	0.07
MgO	12.86	11.40	13.94	13.71	14.59	15.13	14.93	15.73	15.01	15.79	14.55	13.16	13.84	13.39
ZnO	0.00	0.00	0.00	0.00	0.00	0.00	0.00	0.00	0.00	0.00	0.00	0.00	0.00	0.00
CaO	21.86	22.00	22.36	22.09	22.12	22.16	21.89	21.50	21.75	21.63	22.08	21.71	21.73	21.97
Na2O	0.38	0.64	0.50	0.32	0.53	0.48	0.52	0.57	0.54	0.60	0.60	0.50	0.40	0.46
K2O	0.00	0.00	0.00	0.00	0.00	0.02	0.00	0.04	0.00	0.00	0.01	0.04	0.00	0.00
Total	99.01	99.98	100.66	100.63	100.15	100.68	100.41	100.29	99.26	100.17	100.93	98.24	99.74	99.74
Si	1.78	1.70	1.82	1.79	1.86	1.88	1.88	1.91	1.91	1.92	1.86	1.84	1.84	1.80
AlIV	0.22	0.30	0.18	0.21	0.14	0.12	0.12	0.09	0.09	0.08	0.14	0.16	0.16	0.20
Ti	0.08	0.11	0.06	0.07	0.04	0.03	0.03	0.02	0.03	0.02	0.04	0.06	0.05	0.05
AlVI	0.03	0.06	0.07	0.02	0.05	0.05	0.06	0.05	0.07	0.05	0.06	0.09	0.09	0.07
Cr	0.00	0.00	0.00	0.00	0.01	0.01	0.03	0.03	0.03	0.03	0.03	0.01	0.01	0.01
Fet	0.25	0.26	0.19	0.25	0.18	0.17	0.17	0.15	0.15	0.14	0.17	0.19	0.20	0.21
Mn	0.00	0.00	0.00	0.01	0.01	0.01	0.00	0.01	0.00	0.00	0.00	0.00	0.00	0.00
Mg	0.72	0.64	0.76	0.76	0.80	0.82	0.82	0.86	0.83	0.86	0.79	0.74	0.76	0.74
Ca	0.88	0.88	0.88	0.88	0.87	0.87	0.86	0.84	0.86	0.85	0.86	0.88	0.86	0.87
Na	0.03	0.05	0.04	0.02	0.04	0.03	0.04	0.04	0.04	0.04	0.04	0.04	0.03	0.03
Fe3+	0.05	0.06	0.03	0.07	0.03	0.03	0.01	0.00	0.00	0.00	0.01	0.00	0.00	0.04
Fe2+	0.20	0.20	0.16	0.18	0.15	0.14	0.16	0.14	0.15	0.14	0.16	0.19	0.20	0.17
FeO*	6.40	6.34	5.28	5.94	4.86	4.64	5.28	4.67	4.72	4.70	5.20	6.06	6.48	5.41
Fe2O3*	1.73	2.06	1.02	2.35	1.21	1.10	0.37	0.12	0.00	0.05	0.46	0.00	0.05	1.61
Total*	99.18	100.18	100.76	100.87	100.27	100.80	100.45	100.30	99.26	100.18	100.97	98.24	99.75	99.90
Mg/Mg+Fet	0.74	0.71	0.80	0.75	0.81	0.83	0.83	0.85	0.85	0.86	0.82	0.79	0.79	0.78
Q=Ca+Mg+Fe2+	1.81	1.72	1.80	1.81	1.82	1.83	1.84	1.84	1.84	1.85	1.81	1.81	1.83	1.78
J=2Na	0.06	0.09	0.07	0.05	0.08	0.07	0.07	0.08	0.08	0.09	0.08	0.07	0.06	0.07
Wo	47.57	49.44	48.09	46.32	46.77	46.52	46.49	45.65	46.74	45.94	47.25	48.62	47.25	47.80
En	38.92	35.95	41.76	40.00	43.01	43.85	44.32	46.74	45.11	46.24	43.41	40.88	41.76	40.66
Fs	13.51	14.61	10.15	13.68	10.22	9.63	9.19	7.61	8.15	7.82	9.34	10.50	10.99	11.54

Number of cations calculated on the basis of six oxygens. x: xenocryst, ph: phenocryst, c: core, b: rim

0.6 mm. No hydrous minerals such as amphibole, phlogopite, or apatite are present.

Chrysolites are $Fo_{78–81}$. Diopsides ($Wo_{48–47}En_{40–41}Fs_{10–11}$) (Fig. 5) of the clinopyroxenites are Al_2O_3-rich (up to 7.2 wt.%) and contain up to 2.3 wt.% TiO_2 (Table 3). These clinopyroxenes (Mg# = 78 to 79) are very different from those of typical mantle origin (Mg#= 91 to 93) described elsewhere along the CVL (Nana 2001). Spinels are interstitial titanomagnetites. Their FeO_t contents are between 58 and 60 wt.% (Fig. 6, Table 4). Their low Cr_2O_3 contents (4.5 wt.% Cr_2O_3) are one of the major difference that distinguish the spinels of clinopyroxenites from those of dunites (19 to 21 wt.% Cr_2O_3) and wehrlites (22 to 25 wt.% Cr_2O_3). Mg# and Cr# have almost constant values of nearly 25.

Geochemistry of the series

Twenty-six samples of lavas and two xenoliths from the Mount Cameroon have been analyzed. Nine lava analyses have been selected (Table 5) as representative of the alkaline series: three basanites including the host of the xenoliths, two alkali basalts, two hawaiites, and two mugearites. In the TAS diagram (Le Maitre 2002), most of the lavas plot within the basanite, basalt and hawaiite

Table 4 Representative microprobe analyses of microcrysts of spinels from the host basanite and xenoliths

Rock	host basanite			dunite				wehrlite		clinopyroxenite		
Sample	TM190a			TM190b				TM190e		TM190d		
Analysis	195	200	201	52	54	56	58	132	140	72	83	84
TiO2	19.41	22.84	22.01	6.97	6.91	7.08	6.99	4.39	5.06	14.31	15.34	15.52
Al2O3	6.28	4.63	6.27	10.13	10.19	10.26	10.27	18.59	16.80	8.84	9.32	9.22
Cr2O3	2.88	0.45	0.46	19.85	20.20	20.59	20.90	22.69	25.31	4.56	4.52	4.46
FeOt	63.03	65.60	61.82	52.43	52.81	53.59	53.92	41.89	43.32	59.82	57.97	58.06
MnO	0.27	0.83	0.32	0.21	0.39	0.16	0.39	0.19	0.39	0.40	0.31	0.29
MgO	5.01	3.14	3.50	7.32	7.40	7.14	7.18	9.75	9.45	6.17	7.02	6.54
CaO	0.07	0.20	0.21	–	–	0.01	0.02	–	0.04	0.14	0.10	0.08
NiO	0.28	0.06	0.06	0.28	0.14	0.42	0.31	0.37	0.13	0.08	0.08	0.16
Total	97.23	97.75	94.65	97.19	98.04	99.25	99.98	97.87	100.50	94.32	94.66	94.33
Ti	4.12	4.94	4.86	1.43	1.40	1.43	1.40	0.85	0.97	3.05	3.24	3.30
Al	2.09	1.57	2.17	3.25	3.25	3.24	3.22	5.64	5.03	2.95	3.09	3.07
Cr	0.64	0.10	0.11	4.28	4.31	4.35	4.39	4.62	5.08	1.02	1.00	1.00
Fet	14.88	15.77	15.17	11.96	11.94	12.00	11.99	9.02	9.20	14.18	13.60	13.72
Mn	0.07	0.20	0.08	0.05	0.09	0.04	0.09	0.04	0.09	0.10	0.07	0.07
Mg	2.11	1.35	1.53	2.97	2.98	2.85	2.84	3.74	3.58	2.61	2.94	2.76
Ca	0.02	0.06	0.07	–	–	0.00	0.00	–	0.01	0.04	0.03	0.02
Ni	0.06	0.01	0.01	0.06	0.03	0.09	0.07	0.08	0.03	0.02	0.02	0.04
Total	23.99	24.00	24.00	24.00	24.00	24.00	24.00	23.99	23.99	23.97	23.99	23.98
Fe3+	5.02	4.46	4.01	5.61	5.63	5.54	5.60	4.02	3.92	5.85	5.41	5.28
Fe2+	9.87	11.31	11.17	6.35	6.31	6.46	6.40	5.00	5.29	8.33	8.19	8.44
FeO*	41.79	47.07	45.50	27.83	27.91	28.83	28.76	23.21	24.88	35.13	34.90	35.72
Fe2O3*	23.61	20.60	18.14	27.33	27.66	27.51	27.97	20.76	20.49	27.43	25.64	24.84
Total*	99.60	99.82	96.47	99.92	100.80	102.00	102.79	99.95	102.55	97.06	97.23	96.83
Mg/Mg+Fe2+	0.18	0.11	0.12	0.32	0.32	0.31	0.31	0.43	0.40	0.24	0.26	0.25
Cr/Cr+Al	0.24	0.06	0.05	0.57	0.57	0.57	0.58	0.45	0.50	0.26	0.25	0.24
Chromite	0.04	0.01	0.01	0.27	0.27	0.28	0.28	0.29	0.32	0.06	0.06	0.06
Mg-ferrite	0.13	0.07	0.06	0.17	0.17	0.16	0.16	0.12	0.13	0.14	0.18	0.15
Magnetite	0.16	0.18	0.18	0.17	0.17	0.18	0.18	0.13	0.10	0.22	0.15	0.17
Spinelle	0.13	0.10	0.14	0.20	0.20	0.20	0.20	0.36	0.32	0.19	0.19	0.19
Ulvospinelle	0.52	0.62	0.61	0.18	0.18	0.18	0.18	0.11	0.12	0.38	0.41	0.41
Jacobsite	0.01	0.03	0.01	0.01	0.01	0.00	0.01	0.01	0.01	0.01	0.01	0.01

Number of cations calculated on the basis of 24

fields (DI<45) (Fig. 7). The most differentiated lavas (hawaiites and mugearites) were mainly sampled above 2,000 m. The analyzed xenoliths are one dunite and one wehrlite (Table 5).

Basic lavas have typical characteristics of an alkaline series. TiO_2 contents are high (2.4 to 3.4 wt.%), Na_2O contents range between 2.9 and 4.7 wt.% and K_2O between 1.1 and 2.1 wt.%. Note that losses on ignition are far lower than 2 wt.%, corresponding to the upper limit for fresh, unaltered igneous rocks according to Le Bas et al. (1986).

The chemical variations of the lavas are characterized by progressive increase in SiO_2, Na_2O, K_2O and Al_2O_3 and decreasing MgO, CaO and Fe_2O_3 with progressive differentiation (Fig. 8a). Transition element contents (Cr, Ni, Co) decrease with decreasing MgO content in agreement with fractionation of mafic minerals such as olivine (chrysolite) and diopside in the less evolved magmas (Fig. 8b). Fe_2O_3, TiO_2 and V contents are nearly constant and then decrease as differentiation progresses, which attests the crystallization of Fe-Ti oxides occurred during an intermediate stage. Incompatible element contents (K, Rb, Zr, Y) increase with differentiation, while Sr remains roughly constant. The host basanite is characterized by a low Mg# ratio=100 Mg / (Mg + Fe_t) of 56.9 and total alkali of 4.8 wt.%. The CIPW normative composition of this basanite, calculated for Fe_2O_3/FeO ratio of 0.2 according to Middlemost (1989), reveals 12.4 wt.% of nepheline and a DI of 26.8.

The bulk analysis of the dunite (TM190b, Table 5) is very close to those of the olivines (Table 2) which are the main constituents of that rock, as exemplified by very high

Fig. 3 Modal composition (vol.%) of studied xenoliths compared with some other xenoliths founded in Cameroon, in a olivine - orthopyroxene - clinopyroxene triangle. Classification after Streckeisen (1976)

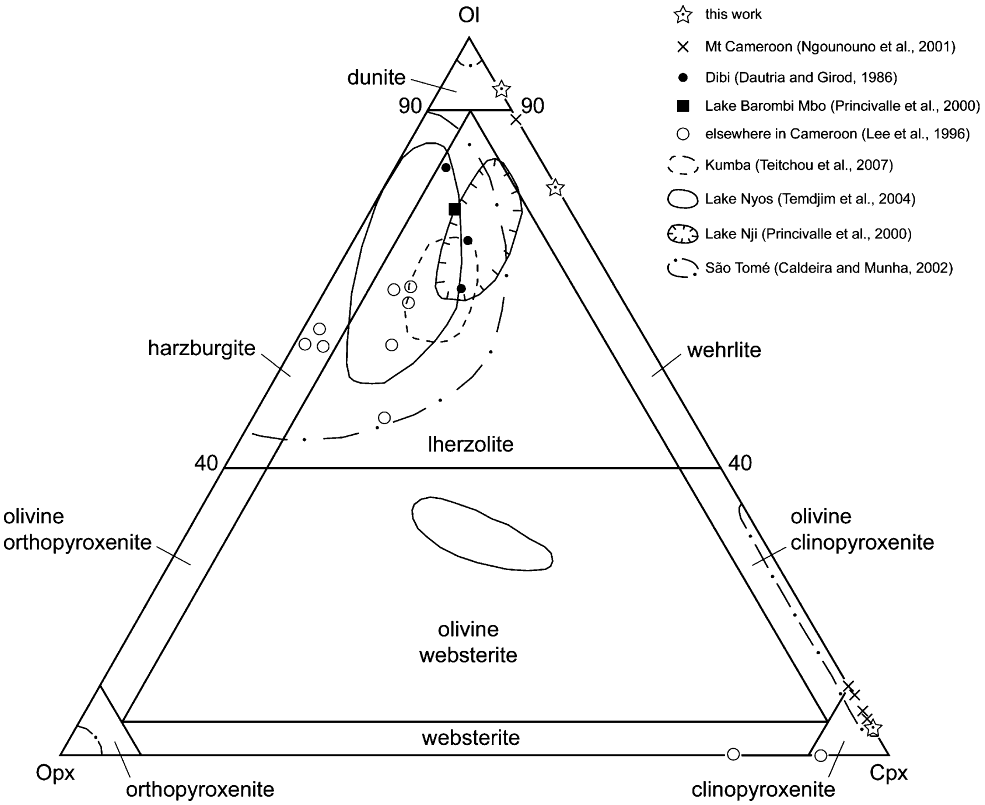

Ni and Cr contents. The bulk composition of the wehrlite (TM190e, Table 5) reflects its modal analysis. This is graphically illustrated (Fig. 9) by a wehrlite composition that plots between those of its olivines and clinopyroxenes. CIPW norm calculation (for Fe_2O_3/FeO ratio of 0.2) for the wehrlite gives 46.1 wt.% of forsterite and 42.7 of diopside and a small amount of oxides, feldspars and feldspathoids, that is to say a ratio (percentage) of 51.9 wt.% of olivine against 48.1 wt.% of diopside. These values are somewhat different from the modal composition (respectively 79 and 21 wt.%) estimated by eye while modal minerals are not pure end-members. Moreover these differences could be linked to some heterogeneities and the small size (0.4–2 mm) of the xenoliths. Mg# ratios are respectively 84.7 and 83.7 for the dunite and the wehrlite. Note that Ni and Cr contents of the wehrlite are about half of those of the dunite.

The trace-element patterns of the studied lavas are all parallel, indicating that the magmas are cogenetic (Fig. 10), and that fractional crystallization was an important process. Note that the dunites and wehrlites are poorer in normalized REE than their host lava and all others lavas of the volcano (i.e. Lu normalized value of 0.15 and 0.63 respectively in the dunite and wehrlite, 4.58 in the host lava). Their lower REE contents and low (Nb/Y) ratios emphasise that they have cumulative origin. These alkaline liquids could have been derived from partial melting of a garnet- rich lherzolite in the upper mantle beneath the Cameroon Volcanic Line as witness by the fractionation of the HREE (Tb, Y, Yb). Then they crystallised at lower pressures the dunites and wehrlites.

In view of the very young ages of the lavas (see below), the measured Sr and Nd isotopic ratios (results obtained by D. Demaiffe at the Laboratoire de Géochimie isotopique, Université Libre de Bruxelles) can be used as initial ratios. The $^{87}Sr/^{86}Sr$ ratios fall in a narrow range (0.703344 and 0.703198 for basanite TM198 and basalt TM1 respectively) as the $^{143}Nd/^{144}Nd$ ratios (0.512773 and 0.512851). These values are similar to those obtained for the lavas of the whole CVL (Halliday et al. 1988) and for most minerals of xenoliths (Lee et al. 1996) and are typical of mantle-derived magmas.

K-Ar ages

Whole rock dating of seven lavas coming from different areas of Mount Cameroon (located in Fig. 2) have been carried out by the K-Ar method: five samples have been dated on whole rock at the Université of Brest and two samples on groundmass at CNRS Gif-sur-Yvette (Table 6). These are the first seven K-Ar data on this volcano.

The ages range from 2.83±0.11 to 0.00±0.09 Ma. The host basanite (TM190a) of the xenoliths has been dated at

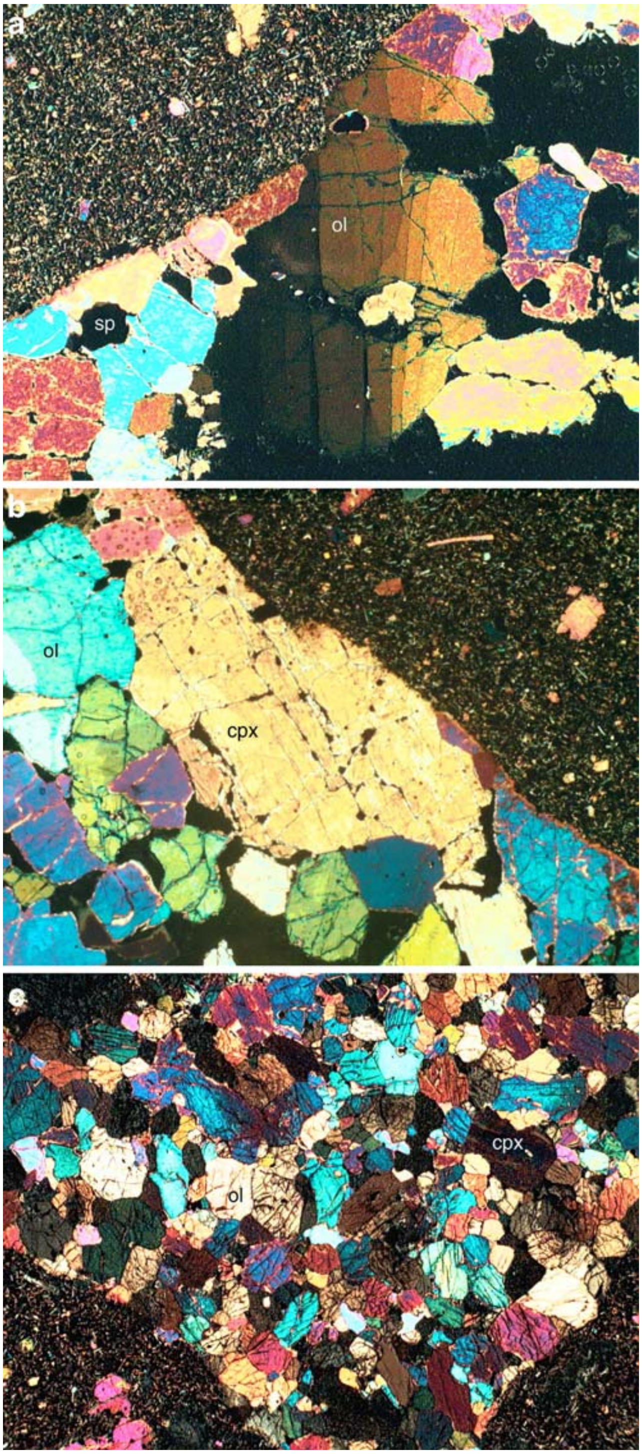

Fig. 4 Texture of the xenoliths. Each picture corresponds to a sector of 5 x 3,8 mm. ol = olivine (chrysolite), cpx = clinopyroxene, sp = spinel. **a** porphyroclastic texture (dunite, TM190b); **b** porphyroclastic texture (wehrlite, TM190e); **c** mosaïc equigranular texture (clinopyroxenite, TM190d)

0.73±0.08 Ma, in the range of the other ages (Table 6). The ages obtained on groundmass are recent (20 ka and 29 ka). Some ages are older than those of Hedberg (1968) who proposed an age of Mount Cameroon of less than 1 Ma.

In fact, Mount Cameroon grew in two major phases:

(1) during the Miocene, which is only known as interstratified basaltic relics in the Burdigalian sediments of the Douala Basin (Gèze 1943, Reyre 1966). The other volcanics of this phase have been covered by the more recent products during important recent activity;
(2) after a long (12–17 Ma) period of rest, a new period of activity started during the middle Pliocene, at nearly 2.8 Ma (Piacenzian) until recent times (ages of 29 to 0 ka) and continues today. Five eruptions (1838, 1852, 1865, 1866, 1868) are noted during the 19th century and seven eruptions (1909, 1922, 1954, 1959, 1982, 1999, 2000) during the 20th century.

The regular and high activity of Mount Cameroon explains the important volume of the volcanic edifice (the highest of the whole Cameroon Line) as well as the weak differentiation of the lavas.

Interpretation and discussion

This study has led the following results:

(1) The host lava is a vesicular, porphyritic basanite, which contains olivine (chrysolite) and diopside as euhedral phenocrysts as well as angular xenocrysts, and chrysolite, diopside, titanomagnetite and plagioclase as microcrysts in the matrix.

The whole rock K-Ar age of the host basanite is 0.73±0.08 Ma (Table 6). Six others lavas have been dated from 2.83±0.11 to 0.00±0.09 Ma. These seven age determinations are the first K-Ar data for Mount Cameroon; they show that Mount Cameroon has been active for the last three millions years, and remains active as shown by important recent eruptions.

The $^{87}Sr/^{86}Sr$ and $^{143}Nd/^{144}Nd$ ratios fall in a narrow range (0.703198 to 0.703344 and 0.512851 to 0.512773 respectively) typical of mantle origin. The Sr-Nd isotopic compositions of Mount Cameroon lavas show that crustal contamination was negligible during ascent and differentiation of the magma.

(2) Three types of xenoliths have been found as inclusions in the host basanite: dunites, wehrlites and clinopyroxenites. They contain three main mineral phases: chrysolite, diopside and spinel. Few such xenoliths have been described from Cameroon. Conversely, xenoliths of spinel lherzolites and olivine websterites are common

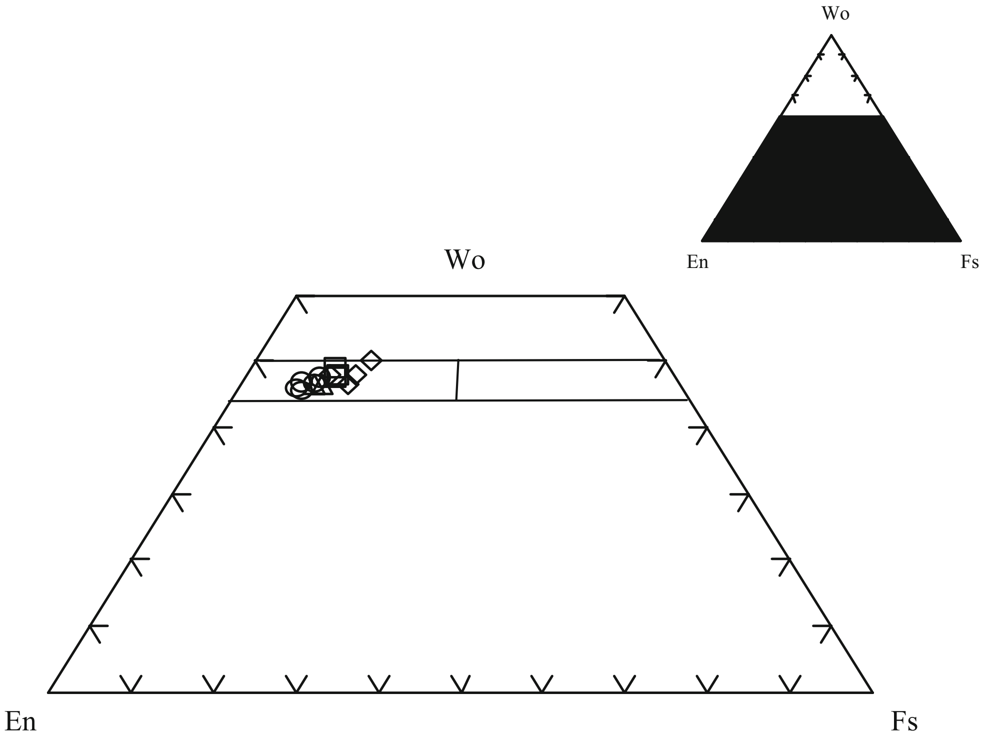

Fig. 5 Clinopyroxene compositions, plotted in the Wo-En-Fs diagram (according to Morimoto 1988). Diamond: host basanite, triangle: dunite, circle: wehrlite, square: clinopyroxenite

along both the oceanic and the continental sectors of the Cameroon Line (Déruelle et al. 1991; Lee et al. 1996; Temdjim et al. 2004). Recently, Teitchou et al. (2007) describe xenoliths that are lherzolites containing 14–26% of orthopyroxene in Kumba Plain, Cameroon.

(i) Mg# of chrysolites in the xenoliths range from $Fo_{83–84}$ in the dunites to Fo_{79} in the clinopyroxenites while Mg# of chrysolite phenocrysts of their host lava range between 75 and 81. These values are far lower than those (91 to 94) of olivines of mantle xenoliths of the CVL that are interpreted as residues of partial melting. In the same way, CaO contents in the chrysolites of the dunites (0.1–0.4 wt.%) and the wehrlites (0.2–0.3 wt.%) are greater than those of chrysolites of mantle origin (0.05–0.1 wt.%) (Lee et al. 1996). This probably indicates equilibration under lower pressure.

(ii) Diopsides of clinopyroxenites are rich in Al_2O_3 (up to 7.2 wt.%) and have TiO_2 contents up to 2.3 wt.%. These values are typical of the alkaline series (Kushiro 1960). Al^{IV}/Al^{VI} ratios are quite high (5 to 10.5) in the clinopyroxenes of the host basanite but lower (1.2 to 4.9) in the clinopyroxenes of the xenoliths (Table 3).

(iii) Spinels found in the xenoliths are mostly interstitial and xenomorphic, probably because they crystallized late. They are always Fe- and Ti-rich (40–65 wt.% FeO_t and 4–23 wt.% TiO_2) vs. Mg-poor (3–10 wt.% MgO), sometimes Cr-rich (20–25 wt.% Cr_2O_3, except in those of the clinopyroxenites with 4.5 wt.%) (Table 4, Fig. 6) and contain 9–19 wt.% Al_2O_3. Cr/Cr+Al ranges from 0.05 to 0.58 (Table 4). In this way they are quite different from spinels of typical mantle peridotite, that are usually interstitial, but Cr- and Al-richer, with Al_2O_3 contents quite high (>30 wt.%) according to Babkine et al. (1966).

(iv) All these xenoliths lack orthopyroxene, which is a strong indication that they crystallized from an alkaline magma. Moreover, Mg# ratios of respectively 84.7 and 83.7 for the dunite and the wehrlite are typical of the alkaline series and lower than values of more than 90 that are typical of the tholeiitic series.

(v) Geothermometry calculations based on the chemical composition of olivine (White 2005) give temperatures on the order of 1200°C for the chrysolite phenocrysts of the host basanite. Moreover, the equilibration temperatures of xenoliths have also been estimated using Mg/Fe^{2+} partitioning between olivine and spinel (Fabriès 1979). The estimated late equilibrium temperatures range between 690°C and 700°C for the dunite and between 726°C and 765°C for the wehrlite. These temperatures are similar (750–850°C) to those obtained on ultramafic xenoliths (spinel lherzolites with minor dunites and wehrlites) from Tahiti (Tracy 1980).

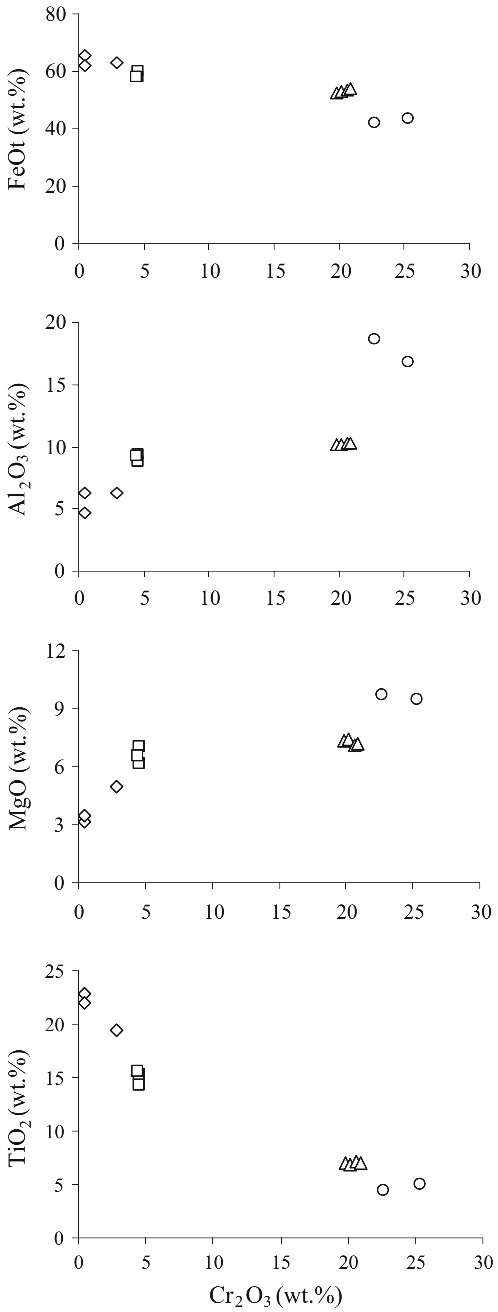

Fig. 6 Diagram for oxides contents vs. Cr_2O_3 of spinels (same symbols as Fig. 5)

(3) These results enable us to discuss three hypotheses for the origin of these xenoliths:

  (i) they are the solid residues of a mantle of lherzolitic composition, which are common along the CVL (Nana 2001).
  (ii) they may be products (cumulates) of fractional crystallization of a liquid of similar chemical composition as the host basanite.
  (iii) or they may have crystallized (cumulates) from an earlier magma and were picked up by a younger magma on his way to the surface.

Mg# ratios of dunite and wehrlite of 83–85 are significantly lower than those of lherzolites (89–90) described by Teitchou et al. (2007), which appear to be similar to those of primitive mantle (88.7–90.1 according to GERM (Geochemical Earth Reference Model) internet site: http://www.earthref.org).

The presence of interstitial chromian spinel (Cr# between 45 and 58) with relatively high TiO_2 contents (between 4 and 7 wt.%) in the dunite and wehrlite, exclude the hypothesis (i) that the xenoliths are the solid residue of mantle. According to Cr# Sp vs Mg# Ol discriminating compositions of peridotites (Arai 1992), the dunite and the wehrlite analyses strongly depart from the OSMA (Olivine-Spinel Mantle Array) (Fig. 11).

More generally, the characteristics of Mount Cameroon xenoliths differ of those resulting from a solid residual mantle as reported by Caldeira and Munha (2002) on Sao Tome Island (Mg#>90 and NiO>0.36 wt.% for olivines, Mg#>90 and TiO_2<0.06 for clinopyroxenes), by Temdjim et al. (2004) at Lake Nyos (Mg# of 89–91 for olivines) and by Teitchou et al. (2007) in the xenoliths of Kumba Plain in Cameroon (Mg# of 89–90 for olivines, Al^{IV}/Al^{VI} between 0.6 and 0.8 for the clinopyroxenes). In the same way, diopsides of the clinopyroxenes have Mg# of 78 to 79, very different from Mg# values of 91 to 93 of clinopyroxenes of typical mantle origin described elsewhere along the CVL (Nana 2001). The higher values of Al^{IV}/Al^{VI} (1.2 to 4.9) in the clinopyroxenes of the xenoliths of Mount Cameroon compared to the equilibrium of the clinopyroxenes of the mantle peridotites of Kumba Plain close to Mount Cameroon indicate that they were emplaced at a lower pressure. Spinel of dunites of Mount Cameroon have Cr# and Mg# of respectively 20 and 30, against 9 to 14 and 74 to 78 in Kumba.

Chemical compositions of mineral phases of the dunites and wehrlites are systematically different than those of the basanitic host: (a) olivines are more magnesian, (b) Al^{IV}/Al^{VI} ratios are systematically lower in the clinopyroxenes of the xenoliths, and (c) spinels are richer in Al. This indicates that they were crystallized from an early alkaline magma (hypothesis iii). Reversely, chemical compositions of spinels of clinopyroxenites are very close to those of the host basanite (Fig. 6). Moreover there is a significant gap between the spinel compositions of dunite and wehrlite on one hand and of clinopyroxenite and host basanite on the other hand. In the same way, olivines of dunites (Fo_{83-84}) and wehrlites (Fo_{81-84}) are nearly the same, and are more magnesian than those of clinopyroxenites (Fo_{78-81}) and host basanite (Fo_{75-81}).

Table 5 Whole rock chemical composition of the host lava compared to the other representative lavas from Mount Cameroon and of two xenoliths (TM190b dunite and TM190e wehrlite) (analyses CRPG, Nancy, France)

	host basanite	basanite		basalt		hawaiite		mugearite		xenoliths	
Sample	TM190a	TM198	TM204	TM130	TM75	TM288	TM289	TM272	TM291	dunite TM190b	wehrlite TM190e
wt.%											
SiO2	43.04	45.32	44.04	46.75	45.39	47.01	47.67	51.86	50.50	38.75	45.23
TiO2	3.23	2.94	3.35	3.14	3.29	3.39	3.01	2.38	2.64	0.16	0.57
Al2O3	13.57	16.29	15.75	14.99	15.09	16.52	16.94	17.82	17.33	0.73	2.06
Fe2O3t	13.91	11.52	12.93	12.39	12.75	12.55	11.31	8.73	10.05	16.08	11.10
MnO	0.21	0.18	0.21	0.17	0.19	0.18	0.19	0.15	0.18	0.21	0.16
MgO	9.28	5.91	6.09	6.58	6.61	4.83	4.47	3.27	3.82	45.09	28.72
CaO	11.18	10.43	11.07	10.66	11.43	9.94	9.45	6.99	7.72	0.69	11.80
Na2O	3.41	4.72	3.87	3.35	3.02	3.72	4.56	4.68	5.19	<l.d.	0.27
K2O	1.43	2.07	1.85	1.19	1.11	1.61	1.70	2.97	2.02	<l.d.	<l.d.
P2O5	0.75	0.63	0.72	0.40	0.52	0.52	0.62	0.58	0.62	<l.d.	0.03
LOI	−0.01	−0.01	0.60	0.31	0.38	−0.32	0.11	0.55	−0.09	−1.29	−0.61
Total	100.00	100.00	100.48	99.93	99.78	99.95	100.03	99.98	99.98	100.42	99.33
ppm											
Ba	471.9	589.5	546.3	340.9	367.4	385.4	529.3	693.5	552.7	<l.d.	3.558
Rb	39.16	52.67	45.44	23.87	22.74	33.32	47.92	70.59	48.35	<l.d.	<l.d.
Sr	1078	1132	1169	744.5	830	835.7	1014	1013	952	7.346	49.60
Y	31.58	32.58	31.09	29.23	29.41	31.02	34.91	37.57	36.78	0.604	4.555
Zr	427.0	435.4	411.8	302.5	307.2	351.0	386.4	576.6	516.4	5.694	20.06
Nb	101.0	110.7	109.7	62.17	68.36	72.55	94.94	117.0	103.3	0.896	1.003
Th	9.003	10.26	9.952	5.466	5.652	6.759	8.621	13.89	10.31	0.085	0.101
Pb	4.2275	5.2475	4.7738	2.7222	2.4284	4.2960	4.0311	8.9283	4.7848	<l.d.	<l.d.
Ga	22.80	25.29	23.93	23.62	23.70	24.98	24.46	27.94	26.18	2.537	3.754
Zn	130.4	120.1	136.5	129.2	120.3	138.5	133.3	120.5	123.5	100.5	63.44
Cu	67.36	63.00	60.91	67.60	55.64	24.35	31.60	27.83	35.39	<l.d.	6.509
Ni	159.4	59.18	51.10	105.1	73.11	22.61	17.20	18.73	12.03	1374	769.2
V	287.4	263.1	283.0	285.8	295.5	308.2	243.3	188.3	182.4	44.4	88.43
Cr	326.3	89.06	49.50	215.8	207.8	18.34	22.13	16.39	11.91	5774	2989
Hf	8.586	8.350	8.612	6.492	6.981	7.511	8.094	11.10	10.18	0.136	0.714
Cs	0.493	0.581	0.523	0.216	0.254	0.443	0.449	0.996	0.529	<l.d.	<l.d.
Ta	7.281	7.601	8.169	4.631	4.937	5.378	6.910	8.112	7.634	0.068	0.096
Co	50.75	36.53	37.36	44.78	42.57	36.46	30.81	21.66	24.55	166.5	91.06
Be	2.055	2.426	2.055	1.389	1.542	1.752	1.926	2.968	2.388	<l.d.	<l.d.
U	2.380	2.475	2.552	1.293	1.485	1.743	2.300	3.571	2.777	0.029	<l.d.
W	0.976	1.228	1.172	0.646	0.664	0.632	1.065	1.248	0.925	<l.d.	<l.d.
Sn	2.387	2.488	2.512	2.263	2.328	2.464	2.403	3.325	2.912	<l.d.	0.524
Mo	3.74	4.09	4.07	1.84	2.04	2.93	4.09	4.25	3.27	<l.d.	<l.d.
La	84.61	89.72	90.02	49.78	55.54	57.12	81.58	96.90	85.64	0.795	2.62
Ce	173.6	175.5	177.8	101.0	113.3	119.3	163.2	193.1	171.1	1.748	7.858
Pr	20.01	19.41	20.04	12.07	13.82	14.50	18.67	21.67	19.52	0.217	1.245
Nd	75.65	70.61	74.18	47.34	54.14	57.50	70.49	80.37	73.16	0.918	6.019
Sm	12.97	12.20	12.64	9.313	10.49	10.71	12.67	13.93	13.09	0.18	1.512
Eu	3.910	3.670	3.762	2.981	3.236	3.347	3.869	4.072	3.938	0.057	0.487
Gd	9.895	9.286	9.616	8.136	8.503	8.915	10.09	10.60	10.33	0.152	1.427
Tb	1.327	1.283	1.312	1.131	1.189	1.233	1.399	1.456	1.433	0.023	0.204
Dy	6.885	6.718	6.743	6.037	6.280	6.521	7.398	7.608	7.550	0.124	1.087
Ho	1.142	1.162	1.131	1.061	1.093	1.112	1.286	1.323	1.315	0.022	0.176
Er	2.860	2.936	2.893	2.648	2.685	2.838	3.310	3.364	3.444	0.066	0.441
Tm	0.379	0.397	0.388	0.358	0.360	0.382	0.447	0.468	0.462	<l.d.	0.055
Yb	2.311	2.457	2.421	2.224	2.209	2.343	2.724	2.950	2.944	0.068	0.336
Lu	0.339	0.362	0.356	0.318	0.320	0.351	0.394	0.426	0.431	0.011	0.047

LOI loss on ignition. l.d. limit of detection

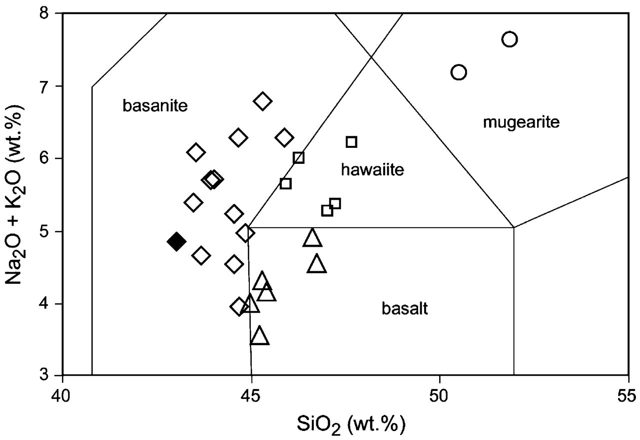

Fig. 7 Total alkalies versus silica plots for the studied lavas (according to *Le Maître* 2002). Full diamond: host basanite

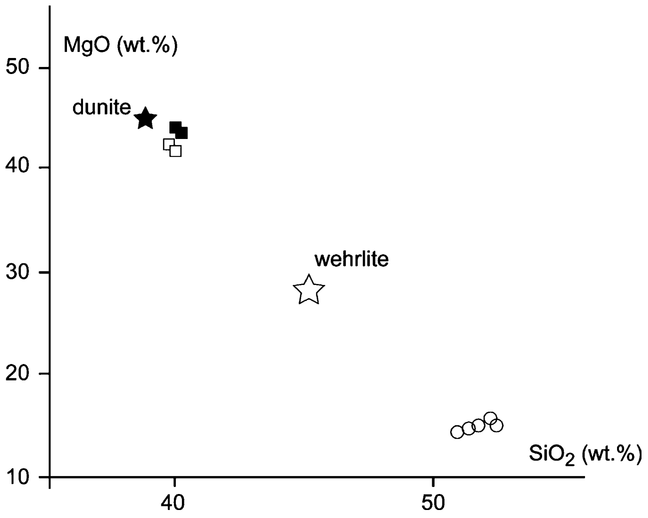

Fig. 9 Comparative bulk rock xenolith and mineral compositions plotted in a MgO vs SiO$_2$ diagram: wehrlite (open star) and its clinopyroxenes (open circle) and olivines (open square); dunite (full star) and its olivines (full square)

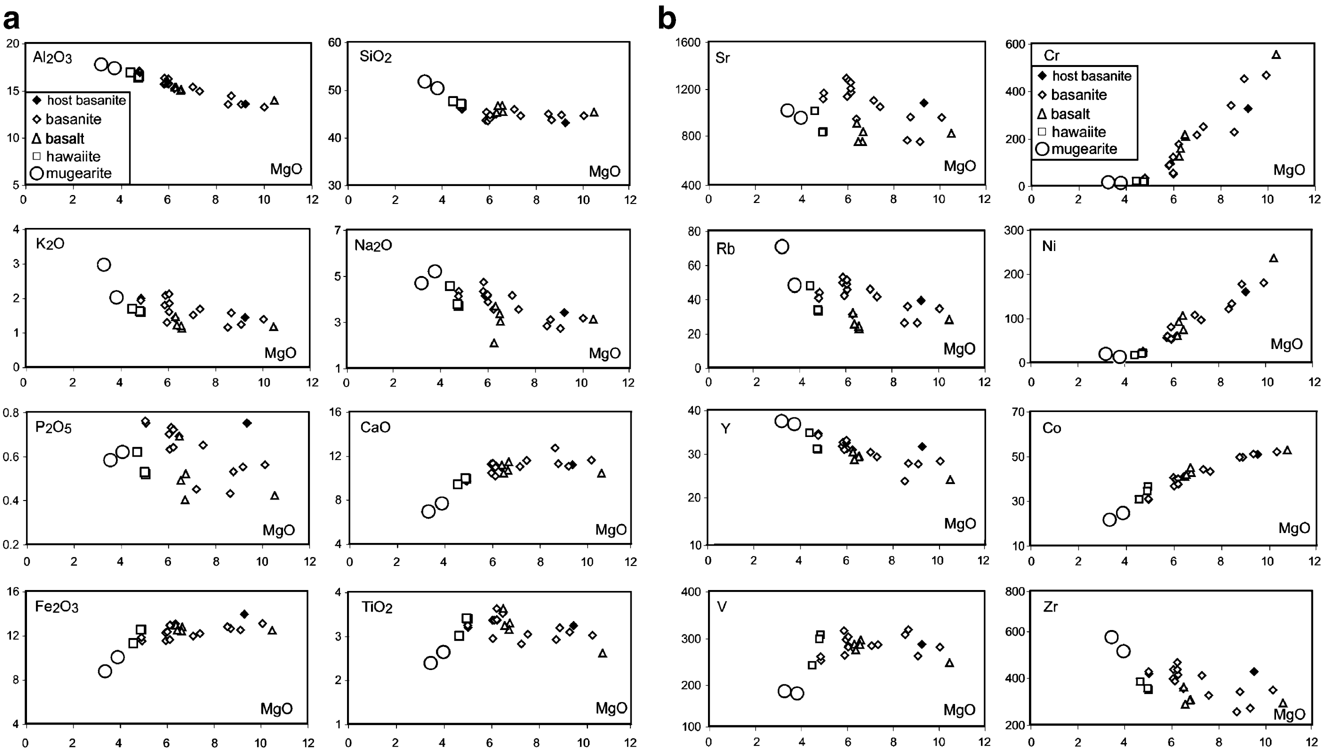

Fig. 8 **a** Major element contents (wt.%) of lavas vs. MgO (wt.%) contents, **b** Trace element contents (ppm) of lavas vs. MgO (wt.%) contents

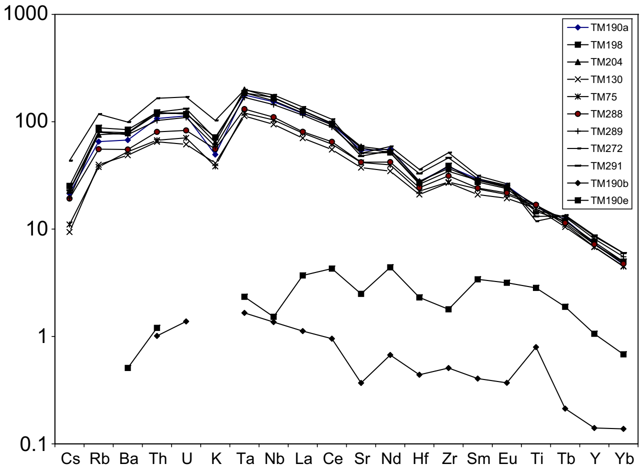

Fig. 10 Primitive mantle-normalised trace element patterns for lava samples and xenoliths from Mount Cameroon. Normalising values from McDonough and Sun (1995). Sample numbers are the same than in Table 5 (TM190b is dunite and TM190e is wehrlite). The nine lava samples have very similar patterns; below are the patterns of wehrlite (square) and of dunite (diamond)

Clinopyroxenite xenoliths are therefore cumulates formed during an early fractional crystallization which may have occurred before the crystallization of the phenocrysts of the host basanite, typically of alkaline affinities. Dunite and wehrlite xenoliths seem to be cumulates that have crystallized from a previous more primitive batch of alkaline magma, with more or less different physical and chemical characteristics, that crystallised beneath the surface and were entrained in a younger eruption of magma of a different composition.

Such a mechanism of emplacement of xenoliths (cumulate type) had been discussed by Vilminot (1965) in Devès Massif, France, Babkine et al. (1966) and Upton et al. (2000) at Réunion Island (Table 7), and Giannetti (1982) at Roccamonfina volcano, Italy. The higher value of Mg# (78 to 84) of olivines in the xenoliths and the lower value (75 to 81) in the phenocrysts show that the xenoliths have crystallized at higher temperatures than the phenocrysts. In the same way, the ratio Al^{IV}/Al^{VI} in the diopsides of the xenoliths is lower than those of the diopsides of the host basanite, suggesting that the xenoliths crystallized under higher pressures (Wilkinson 1975; Wilshire and Shervais 1975). The pressure in the magma chamber has been calculated at 1.0–1.3 GPa (10–13 kbar) using the clinopyroxene-liquid thermobarometer of Putirka et al. (2003) for the host basanite. This corresponds to a depth of 37 to 44 km according to the relationship between depth and pressure: depth (km)=3.02 P(kbar) + 5 assuming a crustal thickness of 30 km with density of 2.8 and a mantle density

Table 6 K-Ar ages of some lavas from Mount Cameroon (Whole rock, Université de Bretagne Occidentale, Brest; Groundmass, CNRS, LSCE, Gif-sur-Yvette)

whole rock

Sample	experiment	rock	place	K_2O (wt %)	molten mass (g)	$^{40}Ar^*/^{40}Ar_T$ (%)	$^{40}Ar^*$ (10^{-7} cm^3/g)	age±1 σ (Ma)
TM1	B6661	alkaline basalt	near Bomana	1.37	1.0032	27.0	1.249	2.83±0.11
TM106	B6664	alkaline basalt	Debundscha Cape	0.97	1.0072	7.9	0.241	0.77±0.09
TM145	B6681	basanite	North East of Limbe	1.23	1.0020	0.0	0.000	0.00±0.09
TM190a	B6625	basanite	North East of Batoke	1.24	1.0023	8.8	0.292	0.73±0.08
TM404	B7015	basanite	East of Mount Cameroon	1.86	0.5453	9.1	0.805	1.34±0.14

groundmass

sample	experiment	rock	place	K_2O±2 σ (wt %)	molten mass (g)	$^{40}Ar^*/^{40}Ar_T$ (%)	$^{40}Ar^*$±1 σ (10^{-14} mol./g)	weighted mean $^{40}Ar^*$±1 σ (10^{-14} mol./g)	age±2 σ (ka)
TM198	7597	basanite	Limbe	1.790±0.018	1.00024	0.753	5.661±0.684		
	7614	basanite	Limbe	1.790±0.018	2.51236	0.830	7.869±0.277	7.558±0.26	29±2
TM407	7661	alkaline basalt	near Munyenge	1.700±0.017	1.04006	0.987	4.639±0.693		
	7677	alkaline basalt	near Munyenge	1.700±0.017	2.35904	1.411	4.916±0.444	4.836±0.374	20±3

Sample are located in Fig. 2. Ages are given in Ma for whole rock analyses and in ka for groundmass analyses. $^{40}Ar_T = {}^{40}Ar^* + {}^{40}Ar_{atmospheric}$

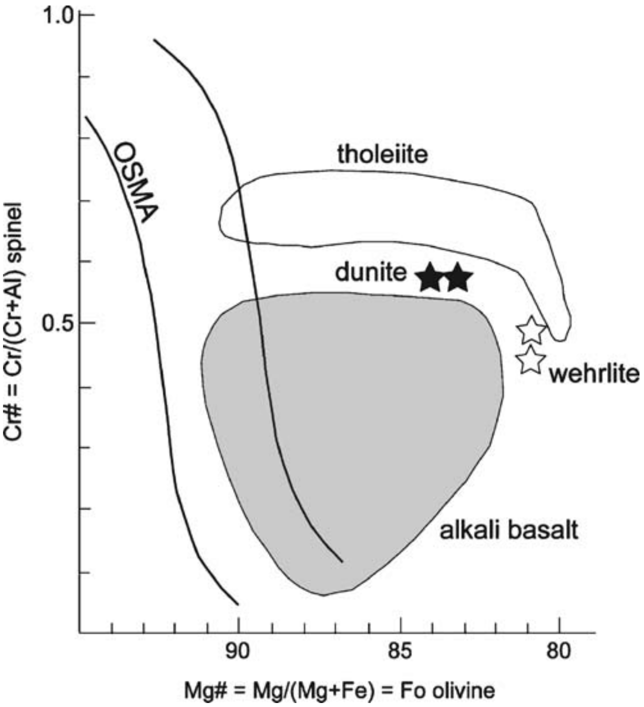

Fig. 11 Cr# of spinel versus Mg# (Fo) of olivine for dunites and wherlites compared to values for intraplate basalts (tholeiites and alkali basalts) and OSMA (Olivine-Spinel Mantle Array) (following Arai 1992)

of 3.3 for depths more than 30 km (Scarrow and Cox 1995).

Déruelle et al. (2001) and Ngounouno et al. (2001) report the presence of frozen basaltic liquids as veins in the xenoliths of wehrlites and pyroxenites sampled at 3,000 m above sea level on the North West of the Mount Cameroon. They propose a mantle metasomatism hypothesis to explain the relatively iron-rich olivine (Fo_{82-85}) according to Bodinier et al. (1991). However, there is no evidence for metasomatism in the xenoliths of dunites, wehrlites and clinopyroxenites sampled during this work on the south side of the volcano as such veins have not been found.

(4) Main concluding remarks

Petrographic studies show that the Mount Cameroon lavas are essentially mafic and mildly differentiated and form a typical alkaline series.

Dunites, wehrlites and clinopyroxenites are the three petrographic types of xenoliths found in a host basanite.

According to respective Mg# = Mg/(Mg+Fe) ratios and to the occurrence of a gap between mineral compositions, we propose a two stages formation for these xenoliths: (1) dunites and wehrlites and (2) clinopyroxenites from host basanites, all in an alkaline context, as has been described from Mount Cameroon and confirmed by the lack of orthopyroxene.

Table 7 Comparison of whole rock chemical analyses of a xenolith of dunite (1), wehrlite (2) from Mount Cameroon (this study), and of three other ultramafic rocks (cumulates): dunites from Réunion Island (3) (Babkine et al. 1966) and (4) (Upton et al. 2000), pyroxenite from Rocher du Lion, Devès Massif, France (5) (Vilminot 1965). l.d. limit of detection

	xenoliths of Mount Cameroon		cumulates of Réunion Island		cumulate of Rocher du Lion (Devès Massif)
	1	2	3	4	5
SiO_2	38.75	45.23	39.20	38.92	37.95
Al_2O_3	0.73	2.06	0.45	0.64	14.62
Cr_2O_3			0.55		0.05
Fe_2O_3	16.08	11.10	5.90	17.23	7.90
FeO			10.10		5.00
MnO	0.21	0.16	0.14	0.22	0.14
MgO	45.09	28.72	44.00	43.27	15.24
CaO	0.69	11.80	0.35	0.38	15.00
Na_2O	<l.d.	0.27	0.05	0.03	1.28
K_2O	<l.d.	<l.d.	0.05	0.01	0.22
TiO_2	0.16	0.57	0.25	0.14	1.64
P_2O_5	<l.d.	0.03	0.06		0.13
LIO	−1.29	−0.61		−1.22	0.55
Total	100.42	99.33	101.10	99.62	99.72

Acknowledgments This work has been supported by the SCAC (Service de Coopération et d'Action Culturelle de la France au Cameroun) and EGIDE (Centre français pour l'accueil et les échanges internationaux). Isotopic data have been measured by D. Demaiffe at the Laboratoire de Géochimie isotopique, Université Libre de Bruxelles. J.C. Philippet has done most of the K-Ar datings at Université de Bretagne Occidentale. L. Daumas has drawn figures. J. Bébien, B. Bonin, G. Delpech, A.R. McBirney and B. Platevoet are thanked for useful remarks. Careful reviews by A. Moeller, H. Downes and M. Grégoire have greatly improved the manuscript.

References

Arai S (1992) Chemistry of chromian spinel in volcanic rocks as a potential guide to magma chemistry. Mineral Mag 56:173–184

Babkine J, Conquéré F, Vilminot JC (1966) Nodules de péridotite et cumulats d'olivine. Bull Soc Franç Minér Crist LXXXIX:262–268

Bellon H, Rangin C (1991) Geochemistry and isotopic dating of Cenozoic volcanic arc sequences around the Celebes and Sulu Seas. In: Silver EA, Rangin C, Breymann MT et al (ed) Proceedings of the Ocean Drilling Program Scientific Results 124:321–338

Bodinier JL, Menzies MA, Thirlwall MF (1991) Continental to oceanic mantle transition-REE and Sr–Nd isotopic geochemistry of the Lanzo lherzolite massif. J Petrol (special issue "Orogenic lherzolites and mantle processes"):191–210

Burke KC, Whiteman AJ (1973) Uplift, rifting and the break-up of Africa. In: implications of continental drift to the Earth Sciences, Tarling D. H. and Runcorn S. K. Eds.:735–755

Caldeira R, Munha JM (2002) Petrology of ultramafic nodules from São Tomé Island, Cameroon Volcanic Line (oceanic sector). J Afr Earth Sci 34(3–4):231–246

Carignan J, Hild P, Mevelle G, Morel J, Yeghicheyan D (2001) Routine analyses of trace elements in geological samples using flow injection and low pressure on-line liquid chromatography coupled to ICP-MS: a study of reference materials BR, DR-N, UB-N, AN-G and GH. Geostandard Newsletter, J Geostandards Geoanalysis 25, 2–3:187–198

Charbit S, Guillou H, Turpin L (1998) Cross calibration of K-Ar standard minerals using an unspiked Ar measurement technique. Chem Geol 150:147–159

Dautria JM, Girod M (1986) Les enclaves de lherzolites à spinelle et plagioclase du volcan de Dibi (Adamaoua, Cameroun): des témoins d'un manteau supérieur anormal. Bull Minéral 109, 3:275–288

Déruelle B (1982) Risques volcaniques au mont Cameroun. Rev Géogr Cameroun 3(1):33–40

Déruelle B, Moreau C, Nkoumbou C, Kambou R, Lissom J, Njonfang E, Ghogomu RT, Nono A (1991) The Cameroon line: A review. In: Kampunzu AB, Lubala RT (eds) Magmatism in extensional Structural Settings. Springer-Verlag, Berlin-Heidelberg

Déruelle B, Bardintzeff JM, Cheminée JL, Ngounouno I, Lissom J, Nkoumbou C, Etamé J, Hell JV, Tanyileke G, N'ni J, Ateba B, Ntepe N, Nono A, Wandji P, Fosso J, Nkouathio DG (2000) Eruptions simultanées de basalte alcalin et de hawaiite au mont Cameroun (28 mars-17 avril 1999). C R Acad Sci Paris, Sciences de la Terre et des planètes / Earth and planetary Sciences 33:525–531

Déruelle B, Ngounouno I, Bardintzeff JM (2001) Wehrlites et pyroxénites en nodules dans les basaltes du Mt. Cameroon: évidence d'un métasomatisme mantellique. 12th International Conference of the Geological Society of Africa, Yaoundé, Cameroon, 27 March-2 April 2001. J Geos Soc Cameroon 1, 1A:39–40

Déruelle B, Ngounouno I, Demaiffe D (2007) The 'Cameroon Hot Line' (CHL): A unique example of active alkaline intraplate structure in both oceanic and continental lithospheres. C R Geosciences 339, 9:589–600

Dumort JC (1968) Carte géologique de reconnaissance du Cameroun à l'échelle 1/500.000, feuille Douala-Ouest avec notice explicative, 69 p, Imprimerie. Nationale, Yaoundé, Cameroun

Fabriès J (1979) Spinel-olivine geothermometry in peridotites from ultramafic complexes. Contrib Mineral Petrol 69:329–236

Fitton JG, Dunlop HM (1985) The Cameroon line, West Africa, and its bearing on the origin of oceanic and continental alkali basalt. Earth Planet Sci Lett 72:23–38

Fosso J, Ménard JJ, Bardintzeff JM, Wandji P, Tchoua FM, Bellon H (2005) Les laves du mont Bangou: une première manifestation volcanique éocène, à affinité transitionnelle, de la Ligne du Cameroun. C. R. Géoscience 337:315–325

Francis PW (1993) Volcanoes. A planetary perspective, Oxford University Press

Gèze B (1943) Géographie physique et géologie du Cameroun Occidental. Mém Mus Nation Hist nat Paris (N.S.) 17:1–271

Giannetti B (1982) Cumulate inclusions from K-rich magmas, Roccamonfina volcano, Italy. Earth Planet Sci Lett 57, 2:313–335

Guillou H, Carracedo JC, Day S (1998) Dating of the upper Pleistocene-Holocene volcanic activity of La Palma using the unspiked K-ar Technique. J Volc Geoth Res 86:137–149

Halliday AN, Dickin AP, Fallick AE, Fitton JG (1988) Mantle dynamics: a Nd, Sr, Pb and O isotopic study of the Cameroon line volcanic chain. J Petrol 29:181–211

Hedberg JD (1968) A geological analysis of the Cameroon trend, Ph. D. Thesis, Univ. Princeton, N.J,

Kusakabe M, Takashi O, Shigeo A (1989) The lake Nyos gas disaster: chemical and isotopic evidence in waters and dissolved gases from three Cameroonian crater lakes, Nyos, Monoun and Wum. J Volc Geoth Res 39:167–185

Kushiro I (1960) Si-Al relation in pyroxenes from igneous rocks. Am J Sci 258:548–554

Le Bas MJ, Le Maitre RW, Streickeisen A, Zanettin B (1986) A chemical classification of Volcanic rocks based on the total alkali-silica diagram. J Petrol 27:745–750

Lee DC, Halliday AN, Davies GR, Essene EJ, Fitton JG, Temdjim R (1996) Melt enrichment of shallow depleted mantle: a detailed petrological, trace element and isotopic study of mantle-derived xenoliths and megacrysts from the Cameroon line. J Petrol 37, 2:415–441

Le Maitre RW (Ed) (2002) Igneous Rocks, A Classification and Glossary of Terms. (Recommendations of the International Union of Geological Sciences Subcommission on the Systematics of Igneous Rocks), Cambridge University Press, Cambridge, UK, 236 p

McDonough WF, Sun SS (1995) The composition of the Earth. Chem Geol 120(3–4):199–398

Mahood GA, Drake RE (1982) K-Ar dating young rhyolitic rocks: a case study of the Sierra La Primavera, Jalisco, Mexico. Geol Soc Am Bull 93:1232–1241

Ménard JJ, Bardintzeff JM, Moundi A, Wandji P, Ngounouno I, Bellon H (2002) Place du magmatisme transitionnel dans le volcanisme de la Ligne du Cameroun. $19^{\text{ème}}$ Réunion des Sciences de la Terre, Nantes, France, 9–12 avril 2002:243

Mercier JCC, Nicolas A (1975) Textures and fabrics of ultramafic peridotits as illustrated by xenoliths from basalts. J Petrol 16:454–487

Middlemost EAK (1989) Iron oxidation ratios, norms and the classification of volcanic rocks. Chem Geol 77:19–26

Morimoto N (1988) Nomenclature of pyroxenes. Bull Mineral 111: 535–550

Moundi A, Wandji P, Bardintzeff JM, Ménard JJ, Okomo Atouba LC, Mouncherou OF, Reusser E, Bellon H, Tchoua FM (2007) Les basaltes éocènes à affinité transitionnelle du plateau Bamoun, témoins d'un réservoir mantellique enrichi sous la ligne volcanique du Cameroun. C R Geosciences 339:396–406

Nana R (2001) Pétrologie des péridotites en enclaves dans les basaltes alcalins récents de Nyos: Apport à la connaissance du manteau supérieur de la ligne du Cameroun. Thèse Doc. d'Etat, Univ. Yaoundé I, Cameroun, 170 p + annexe

Ngounouno I, Déruelle B, Bardintzeff JM (2001) Wehrlite and clinopyroxenite xenoliths from Mt Cameroon: implications for lithospheric processes. XI European union of geosciences meeting, Strasbourg, 8–12 April 2001. J Conf Abstr 6, 1:474–475

Ngounouno I, Déruelle B, Montigny R, Demaiffe D (2006) Les camptonites du Mont Cameroun, Afrique. C R Geosciences 338: 537–544

Nkouathio DG, Kagou Dongmo A, Bardintzeff JM, Wandji P, Bellon H, Pouclet A (2008) Evolution of volcanism in graben and horst along the Cenozoic Cameroon Line (Africa): implication for tectonic evolution and mantle source composition. Mineralogy and Petrology 94(3–4):287–303

Princivalle F, Salviulo G, Marzoli A, Piccirillo EM (2000) Clinopyroxene of spinel-peridotite mantle xenoliths from Lake Nji (Cameroon Volcanic Line, W Africa): crystal chemistry and petrological implications. Contrib. Mineral. Petrol. 139:503–508

Putirka KD, Mikaelian H, Ryerson F, Shaw H (2003) New clinopyroxene-liquid thermobarometers for mafic, evolved, and volatile-bearing lava compositions, with applications to lavas from Tibet and the Snake River Plain, Idaho. Am Mineral 88: 1542–1554

Reyre D (1966) Bassins sédimentaire du littoral africain. Union internationale des sciences géologiques. Association des services géologiques africains, 143–161

Scaillet S, Guillou H (2004) A critical evaluation of young (near-zero) K-Ar ages. Earth Planet Sci Lett 220:265–275

Scarrow JH, Cox KG (1995) Basalts generated by decompressive adiabatic melting of a mantle plume: a case study from the Isle of Skye, NW Scotland. J Petrol 36(1):3–22

Steiger RH, Jäger E (1977) Subcommission on geochronology: convention on the use of decay constants in geo- and cosmochronology. Earth Planet Sci Lett 36:359–362

Streckeisen A (1976) To each plutonic rock its proper name. Earth Sci Rev 12:1–33

Suh CE, Sparks RSJ, Fitton JG, Ayonghe SN, Annen C, Nana R, Luckman A (2003) The 1999 and 2000 eruption of mount Cameroon: eruption behaviour and petrochemistry of lava. Bull Volcanol 65:267–281

Teitchou MI, Grégoire M, Dantas C, Tchoua FM (2007) Le manteau supérieur à l'aplomb de la plaine de Kumba (ligne du Cameroun), d'après les enclaves de péridotites à spinelles dans les laves basaltiques. C R Geosciences 339:101–109

Temdjim R, Boivin P, Chazot G, Robin C, Rouleau E (2004) L'hétérogénéité du manteau supérieur à l'aplomb du volcan de Nyos (Cameroun) révélée par les enclaves ultrabasiques. C R Geosciences 336(14):1239–1244

Tracy RJ (1980) Petrology and genetic significance of an ultramafic xenolith suite from Tahiti. Earth Planet Sci Lett 48(1):80–96

Tsafack JPF, Wandji P, Bardintzeff JM, Nkouathio DG (2007) Occurrence of a sedimentary basement under the Mount Cameroon active volcano (Cameroon Volcanic Line). 26th ECGS (European Center for Geodynamics and Seismology) Worshop, Active Volcanism and Continental Rifting (AVCOR-07), Luxembourg, November 19–21, 2007

Upton BGJ, Semet MP, Joron JL (2000) Cumulate clasts in the Bellecombe Ash Member, Piton de la Fournaise, Réunion Island, and their bearing on cumulative processes in the petrogenesis of the Réunion lavas. J Volc Geotherm Res 104:297–318

Vilminot JC (1965) Les enclaves de péridotite et de pyroxénolite à spinelle dans le basalte du Rocher du Lion (Chaîne du Devès, Haute-Loire). Bull Soc Franç Minér Crist LXXXVIII: 109–118

Wandji P, Ménard JJ, Tchoua FM (1994) L'activité hydromagmatique récente dans la plaine du Noun (Ouest Cameroun) et les aléas volcaniques associés. C R Acad Sci Paris, Sér. II 319:417–422

Wandji P, Bardintzeff JM, Ménard JJ, Tchoua FM (2000) The alkaline fassaite-bearing volcanic province of the Noun plain (West-Cameroon). N Jahrb Miner Mh 1:1–14

Wandji P, Bardintzeff JM, Tchoua FM, Déruelle B, Nkouathio DG, Kagou Dongmo A, Itiga Z, Wotchoko P, Chakam Tagheu PJ (2001) Le mont Cameroun (ligne du Cameroun): un laboratoire naturel d'étude des risques et des bienfaits du volcanisme. GSAf 12: geo-environnemental catastrophes in Africa. J Geoscience Soc, Cameroon 1(1A):134–135

White WM (2005) Applications of thermodynamics in geochemistry. P 701. On line textbook. http://www.imwa.info/Geochemie/chapters.HTML

Wilkinson JFG (1975) Ultramafic inclusions and high pressure megacrysts from a nephelinite sill, Nandewar mountains, North-Eastern New South Wales, and their bearing on the origin of certain ultramafic inclusions in alkaline volcanic rocks. Contrib Mineral Petrol 51:235–262

Wilshire HG, Shervais JW (1975) Al-augite and Cr-diopside suite ultramafic xenoliths in basaltic rocks from the western United States. Phys Chem Earth 9:257–272